Supplementary materials

The supplementary materials include Figures S1–S11 and Table S1.

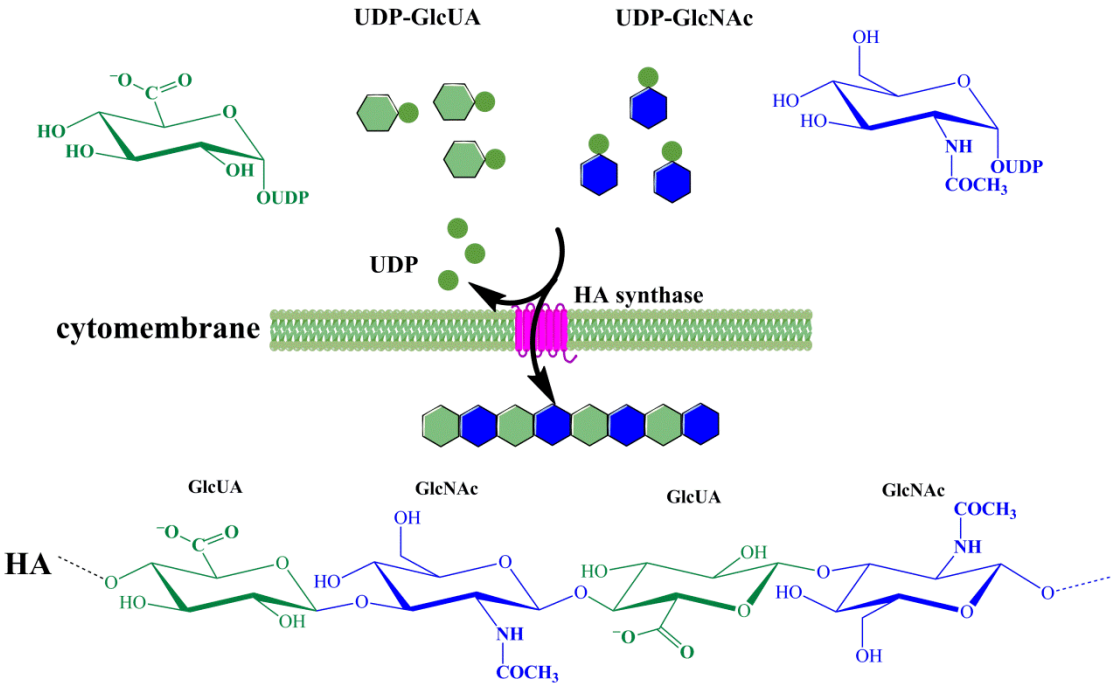

Figure S1. HA formation route *in vivo*. UDP-GlcUA originates from the two-fold oxidation of UDP-glucose. UDP-GlcUA and UDP-GlcNAc are assembled by HA synthase to yield the polysaccharide HA.

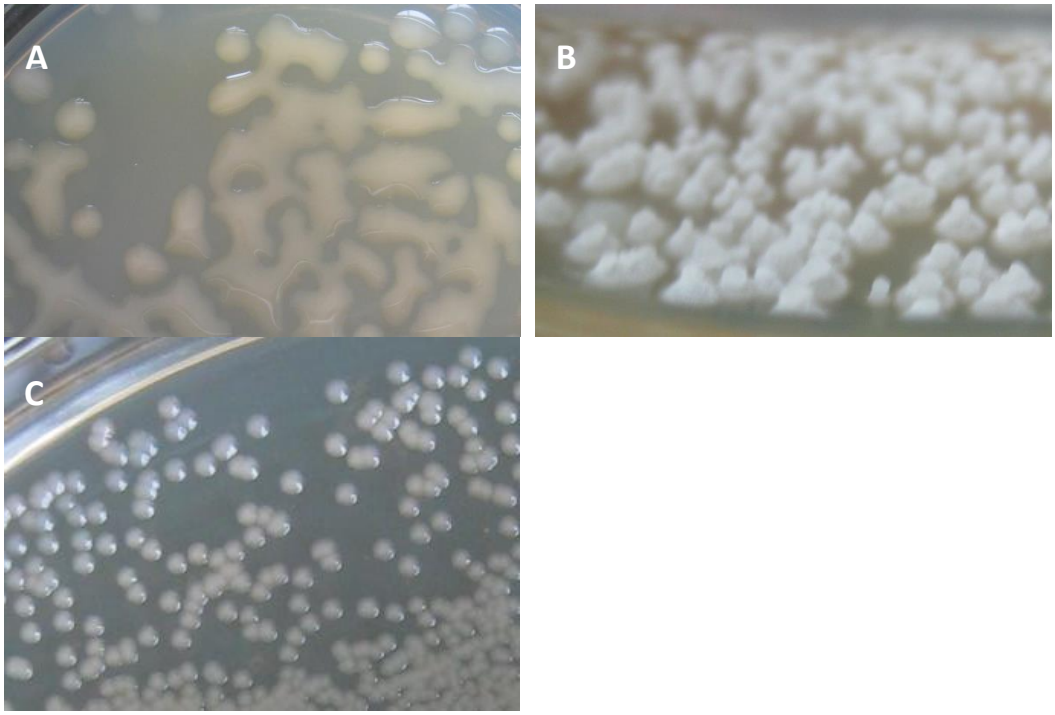

Figure S2. Colony features of the original strain (**S-1**), the electrotransformed strain harboring pKSV7-hasB* (**S-2**), and the single-crossover homologous recombination strain (**S-3**). (A) **S-1** colonies are smooth, subtransparent, and prone to expansion. Vicinal colonies readily merge, generating irregular shapes. (B) **S-2** colonies are coarse, white, and cone-shaped. (C) The **S-3** colonies are smooth, circular, and subtransparent but are not prone to merge.

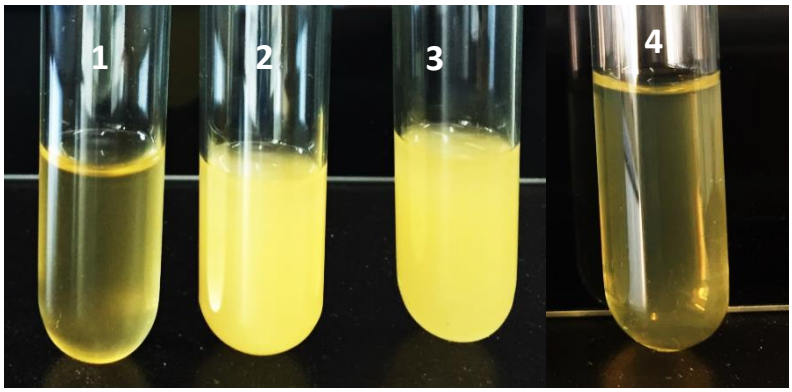

Figure S3. Cultivation media of different strains. The **S-1** medium (1) is relatively clear because the HA product is soluble in water, whereas the **S-2** (2) and **S-3** (3) media are quite turbid, resulting from the product released by the C260A mutant. Notably, the **S-3** medium (4) became significantly clearer after digestion with proteinase K (at 55 ℃ for 12 h).

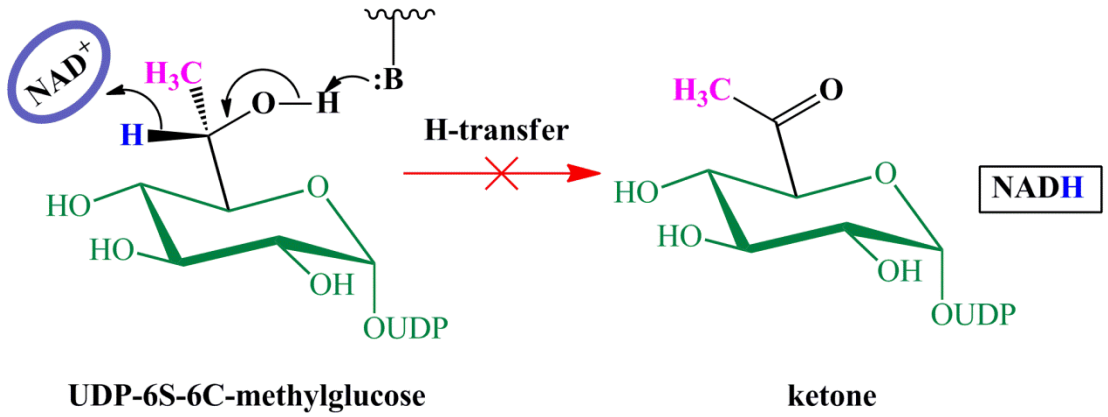

Figure S4. Extremely difficult oxidation of the UDP-glucose analog via a hydride transfer pathway. Even in the presence of 25 mM NH_2OH, which was added to shift the equilibrium toward the ketone product, the value of k_{cat}/K_M for the oxidation of the analog was 10,000 times lower than that for the oxidation of UDP-glucose [21].

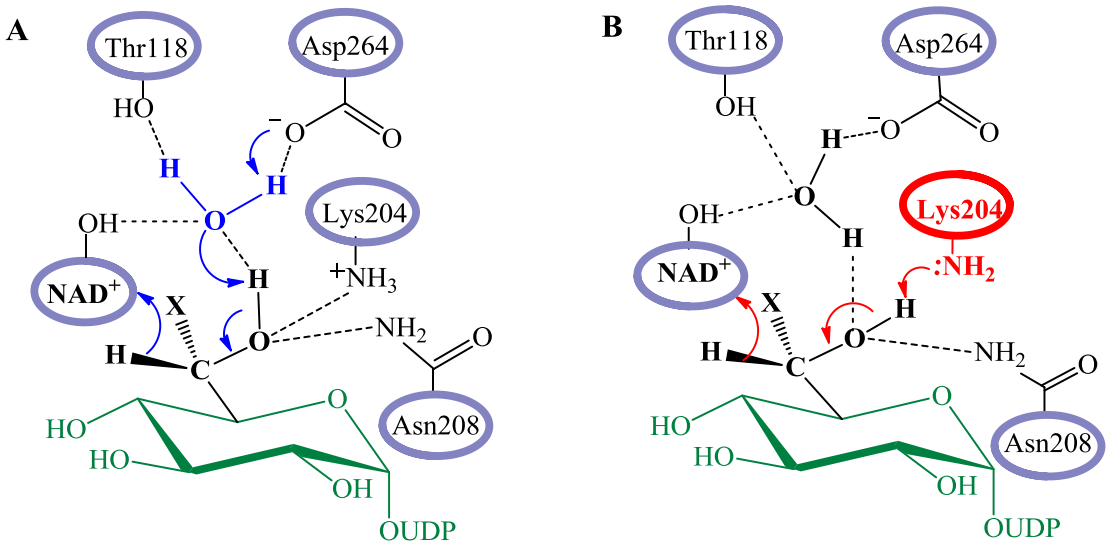

Figure S5. Two possible means of dehydrogenating C6–OH according to previous evidence [30]. X=H for the first oxidation, and X=S–Cys260 for the second. (A) Protonated Lys204–NH_3^+ stabilizes the hydroxyl oxygen atom. A coordinated water molecule acts as the acceptor of the hydroxyl proton. (B) Lys204–NH_2 serves as the acceptor of the C6–OH proton.

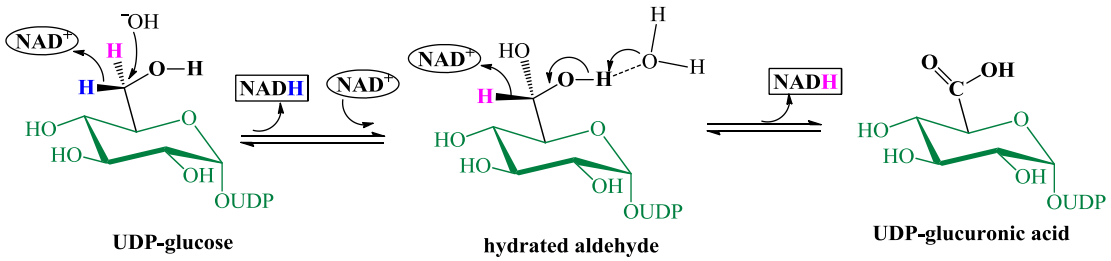

Figure S6. Oxidation of UDP-glucose catalyzed by C260A in the presence of $^{-}$OH. The $^{-}$OH present in solution served as a nucleophile to attack C-6 of UDP-glucose, giving rise to the hydrated aldehyde. The hydrated aldehyde is readily oxidized to the product UDP-glucuronic acid.

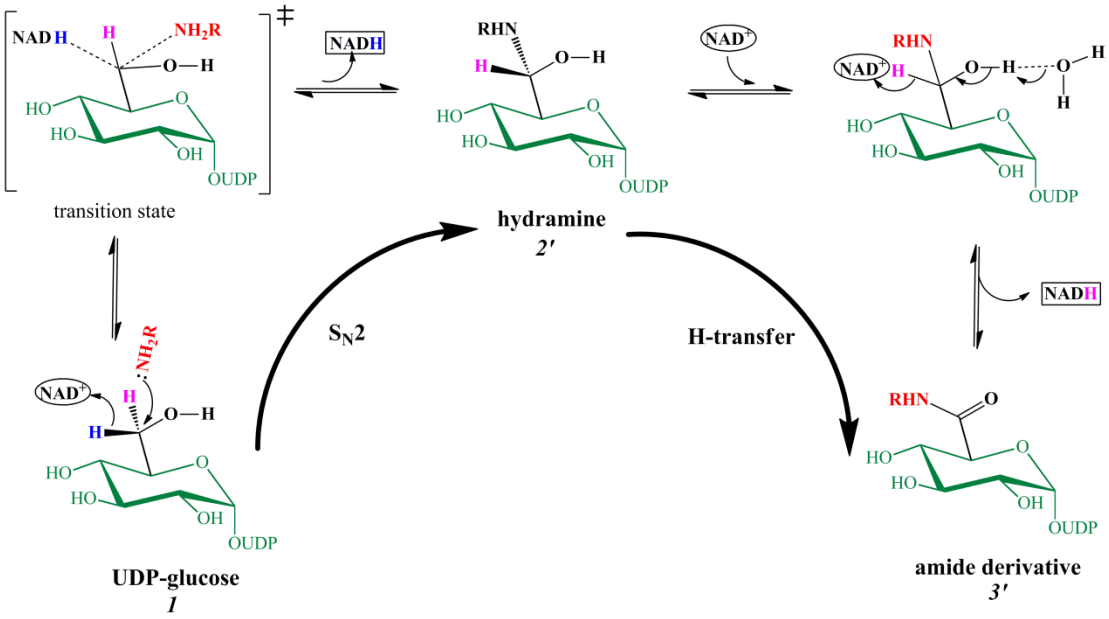

Figure S7. *In vivo* catalysis pathway of C260A. In the absence of Cys260, primary amines (:NH_2R) acting as a nucleophilic reagent initiate the first oxidation. The oxidation of UDP-glucose ***1*** to hydramine ***2′*** is an NAD^+-dependent S_N2 reaction. The second oxidation is a hydride transfer, giving rise to an amide derivative (UDP-Glc-6-amide, ***3′***) of UDP-glucuronic acid. ***3′*** is immediately released into solution due to the absence of this hydrolysis process, which is probably the rate-determining step in the total catalytic mechanism of native UGDH [19].

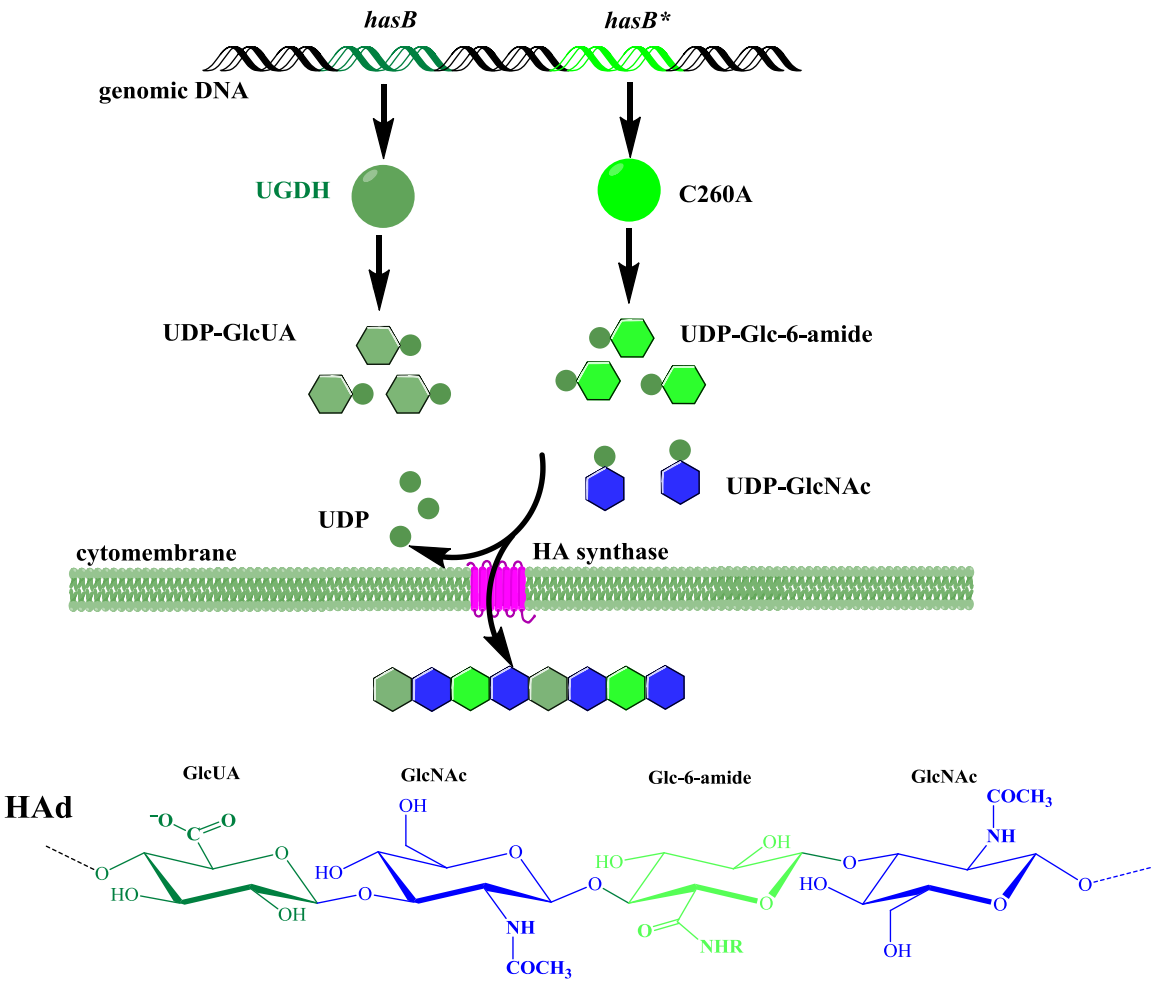

Figure S8. HAd formation route in the **S-3** strain. The amide derivative of UDP-GlcUA (UDP-Glc-6-amide) was generated by C260A and then incorporated into HA by HA synthase to form HAd.

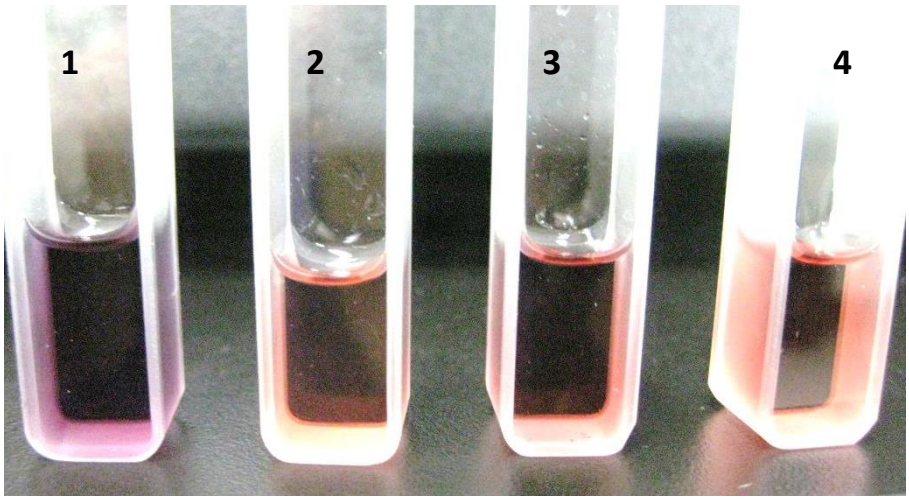

Figure S9. Ninhydrin reaction with HAd or controls. After proteinase K digestion, HAd (1) turned purple. The HAd suspension (2) and the control H_2O (3) did not become purple. The digested solution subjected to purification to remove small molecules, (*e.g.*, amino acid or oligopeptide) (4) did not turn purple. These results demonstrated that HAd does not contain free amino acids and that the primary amine is covalently bound to HA.

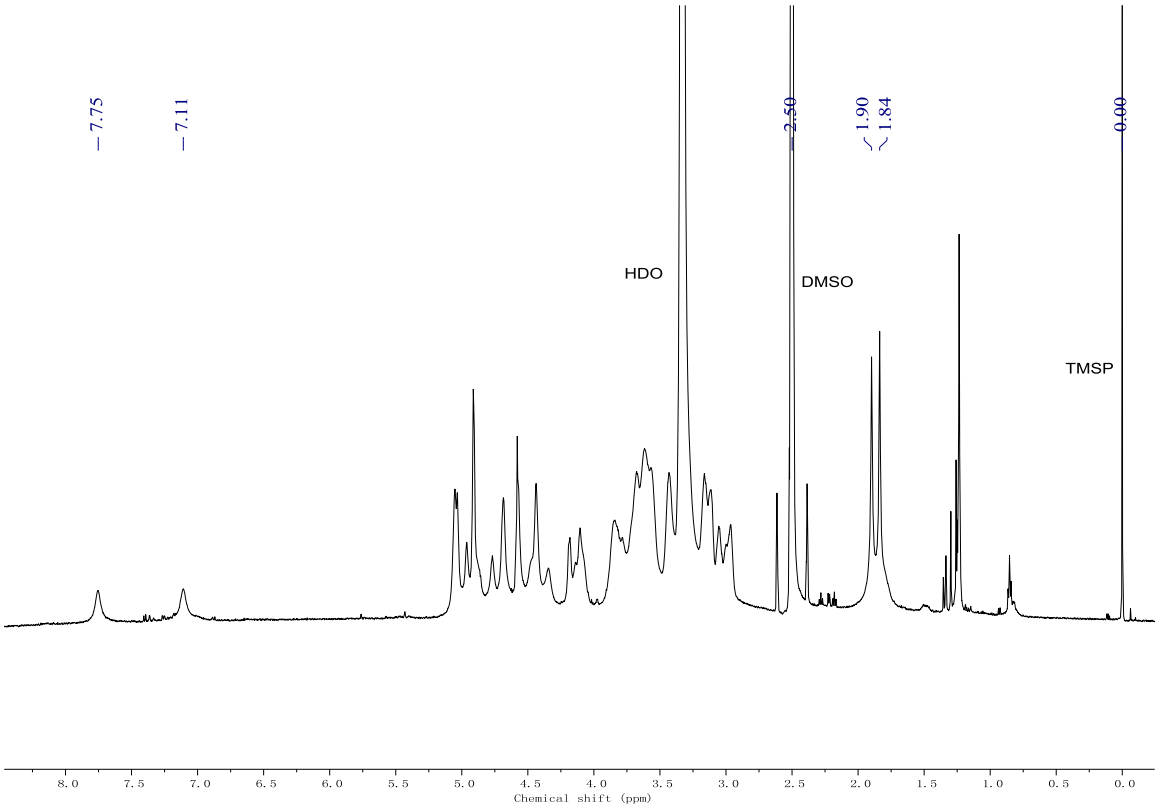

Figure S10. ^{1}H NMR spectrum of fully proteinase K-digested HAd. The solvent is d_6-DMSO. Trimethylsilylpropanoic acid (TMSP) was used as an internal standard. The two peaks at 1.90 and 1.84 ppm should be assigned to the proton of $CH_3CO–$ of GlcNAc. The emergence of two peaks suggests that the incorporation of new groups affects the chemical environment of the acetyl because the –COOH of GlcUA is proximal to the $CH_3CO–$ of GlcNAc in the case of HA. The two short broad peaks at 7.75 and 7.11 ppm should be assigned to amide protons. The former should be assigned to the acetyl of GlcNAc, whereas the latter suggests that a primary amine forms an amide bond with HA.

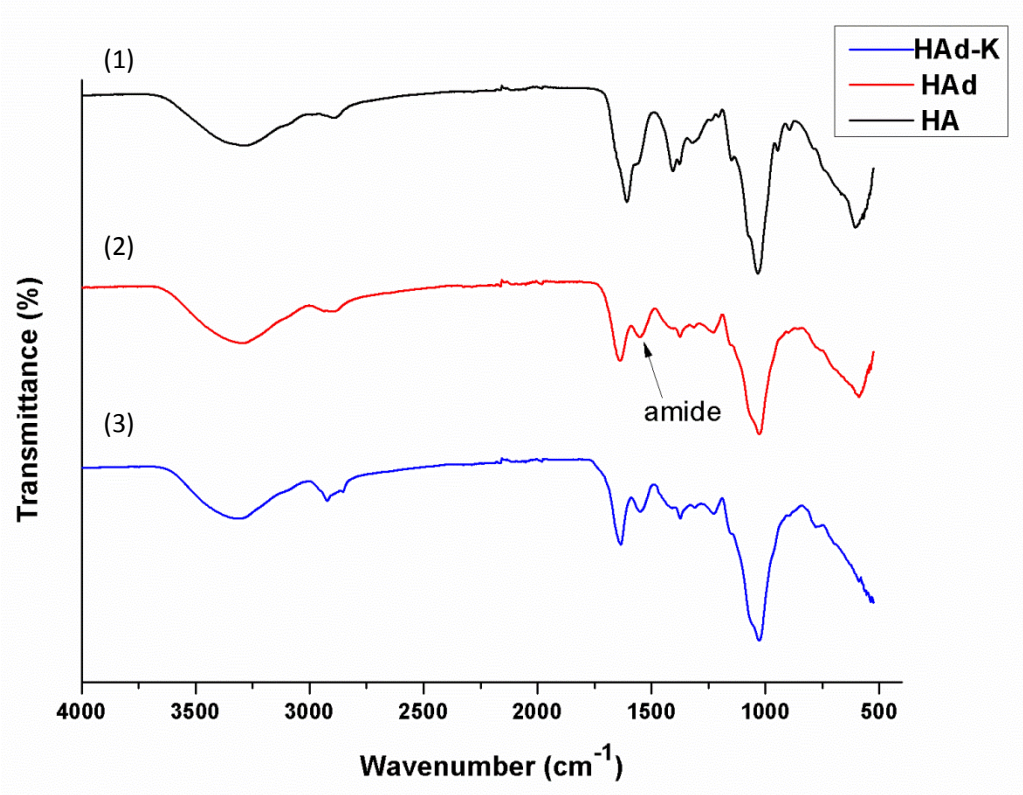

Figure S11. FT-IR spectra of HA and HAd from different processes. (1) HA. (2) HAd: extracted from **S-3** medium. The broad peak at 1568 cm^{-1} should be assigned to the amide as the linkage between the main chain and side chain. (3) HAd-K: proteinase K-digested HAd. HAd-K and HAd have nearly identical characteristic peaks, consistent with the notion that proteinase K neither cuts the main-chain structure of HAd nor digests the amide linkage.

Table S1.

Strains, plasmids, and primers used in this study

Strain, plasmid or primers	Relevant characteristic	References
E. coli DH5α	For cloning exogenous DNA	Sangon
S. zooepidemicus ATCC 39920	Producing HA, labeled **S-1**	ATCC
S. zooepidemicus **S-2**	ATCC 39920 derivative, harboring the plasmid pKSV7-hasB*	This study
S. zooepidemicus **S-3**	ATCC 39920 derivative, single-crossover recombination with pKSV7-hasB*	This study
pUC57	Amp^r	Sangon
pUC57-hasB	pUC57 derivative	This study
pUC57-hasB*	pUC57 derivative	This study
pKSV7	Amp^r, Chl^r, replication at 37 ℃ but not at higher than 41 ℃	Gift from Prof. Wang
pKSV7-hasB*	pKSV7 derivative	This study
hasB-F	GGGGTACCTAGGTTCTGACAAGGGAGC	Amplification of *hasB* fragment
hasB-R	CGGGATCCTGGTCTTCAATAGAGCGTTT	
hasB*-F	CTGTCCTTTGGCAG*GGC*ATGACCGCCATATCCA	For site-directed mutagenesis of *hasB*
hasB*-R	TGGATATGGCGGCTAT*GCC*CTGCCAAAGGACAG	